Resonances that originate from shadow poles of the scattering matrix in multiphoton processes

Martin Dörr and R. M. Potvliege*
Department of Physics, University of Southern California, Los Angeles, California 90089-0484
(Received 13 September 1989)

We have calculated solutions of the Floquet equations for the photodetachment of an electron bound in a one-dimensional Gaussian potential, by using a discrete basis set that includes continuum waves satisfying appropriate boundary conditions. These different solutions correspond to dominant poles or to shadow poles of the scattering matrix; they originate from bound-state solutions in the zero-field limit. We show that one of the "extra" resonances found in a previous complex-coordinate calculation [J. N. Bardsley, A. Szöke, and M. J. Comella, J. Phys. B **21**, 3899 (1988)] can be traced to a shadow pole of one of the bound states of the zero-field system. This example provides further evidence that shadow poles may play an unforeseen and possibly important role in multiphoton processes.

I. INTRODUCTION

A bound state or a resonance of a system is represented by a pole of the scattering matrix. As a function of the energy, the scattering matrix is defined on a Riemann surface consisting of 2^N sheets, where N is the number of channels. In its physically realizable bound states, the system has a (negative) real energy on a particular sheet, the "physical" sheet; the real axis on this sheet is called the "physical" energy axis. A pole of the scattering matrix has an observable effect only if it lies close to or on the physical energy axis; we call such poles the "dominant" poles. It has been known for a long time, in the context of elementary particle physics,[1] nuclear physics,[2] and atomic physics,[3] that each dominant pole is accompanied by a family of "shadow" poles lying on distant "unphysical" sheets. That shadow poles may play an important role in multiphoton processes was apparently first considered by Ostrovskii;[4] the subject was recently discussed at length by Potvliege and Shakeshaft.[5]

The photodetachment of an electron by a purely monochromatic wave can be reduced to a time-independent problem by making the Floquet ansatz. In the presence of the field, the wave function of the electron is asymptotically a superposition of infinitely many outgoing or ingoing waves, each of them being associated with a specific channel, i.e., with a specific number of absorbed or emitted photons. The "dominant" poles correspond to the usual wave functions for photodetachment: the quasienergy is complex, with a negative imaginary part proportional to the decay rate. The wave functions associated with the closed channels decrease exponentially at large distances, while those associated with the open channels are outgoing and for large distances explode exponentially (like the "Gamow-Siegert waves" for one-channel resonances). In other words, if E_M and $k_M=(2E_M)^{1/2}$ are, respectively, the energy and the wave number of the electron in the Mth channel, its wave function is asymptotically $\exp(ik_M x)$, for $x>0$, in the case of a short-range one-dimensional binding potential. With $\mathrm{Im}(E_M)<0$, the branch of the square-root function is such that $\mathrm{Im}(k_M)>0$ [i.e., $\pi/4<\arg(k_M)<3\pi/4$] if $\mathrm{Re}(E_M)<0$, or $\mathrm{Im}(k_M)<0$ [i.e., $-\pi/4<\arg(k_M)<0$] if $\mathrm{Re}(E_M)>0$. However, solutions to the Schrödinger equation obeying other boundary conditions [$\mathrm{Im}(k_M)<0$ for at least one closed channel M, or $\mathrm{Im}(k_M)>0$ for at least one open channel, when $\mathrm{Im}(E_M)<0$] might also exist: these correspond to the "shadow" poles of the scattering matrix.

Frequently, shadow poles have no physical relevance. However, in multiphoton processes, a pulsed laser has an intensity profile, and as the intensity is varied continuously all of the poles move. For example, let us take the case of a dominant pole passing downwards through the Mth photodetachment threshold as the intensity increases: the Mth channel becomes closed as the threshold is passed (that is, the minimum number of photons required for ionization becomes $M+1$), but the wave number k_M does not jump from $\mathrm{Im}(k_M)<0$ to $\mathrm{Im}(k_M)>0$; instead, we have $\arg(k_M)<-\pi/4$ immediately after the threshold is passed, and the pole becomes a shadow pole. Most of the shadow poles tend to follow (on different sheets) the path of the dominant pole. When the dominant pole passes a multiphoton channel threshold, it moves further away from the physical energy axis, while one of its shadow poles usually moves closer to this axis and thus takes over the role of dominant pole.[5] It might also happen—and we see this below—that a shadow pole moves quite differently from the dominant pole, and independently becomes a dominant pole, thereby giving rise to an additional observable resonance.

In this work we calculate some resonance poles for an electron moving in a one-dimensional model potential in the presence of an intense monochromatic field. The same problem was recently investigated by Bardsley, Szöke, and Comella.[6] They found "extra" quasienergy eigenvalues at certain intensities, which they attributed to the appearance of new bound states supported by the potential at large intensity, as discussed by Bhatt, Piraux, and Burnett.[7] However, these extra dominant poles most probably originate as shadow poles that accompany the zero-field bound state or resonance poles. We show that this is certainly the case for at least one of the poles in the

present example. Bardsley, Szöke, and Comella[6] used a complex-coordinate rotation method for calculating the quasienergies. However, in most cases, one must use angles of rotation very close to 0 or much larger than $\pi/4$ for observing shadow poles with this method [because usually $|\mathrm{Re}(E_M)| \gg |\mathrm{Im}(E_M)|$ for the different channels M], and therefore in practice it is very difficult or even impossible to observe these poles using the complex-coordinate rotation method. In order to find the shadow poles as well as the dominant ones, we used a basis set method in which the boundary conditions are imposed *explicitly*, by including in the set a basis function that behaves asymptotically like $\exp(ik_M x)$, $x>0$, for each channel M. The wave numbers k_M are varied until obtaining self-consistency with the resulting quasienergy. This method is an extension to the multiphoton detachment case of a method introduced by Bardsley and Junker[8] for studying resonances in field-free atomic systems. We note that it is often easier to obtain resonance eigenvalues corresponding to *dominant* poles (when the shadow poles are not sought) by expanding the wave functions on a suitable set of complex basis functions[5,9,10] or by using the complex-coordinate rotation approach (i.e., by imposing the boundary conditions *implicitly*). Our method of calculation is described in Sec. II of this paper (we refer the reader to the paper by Isaacson, McCurdy, and Miller[11] for more details), while our results are reported in Sec. III.

II. METHOD

We consider the case of an electron initially bound by a one-dimensional short-range potential $W(x)$, interacting with a monochromatic spatially independent laser field described by the vector potential $A(t)=A_0\sin(\omega t)$. One can seek solutions to the time-dependent Schrödinger equation (we use atomic units throughout)

$$i\frac{\partial}{\partial t}\Psi(x,t)=\left[-\frac{1}{2}\frac{\partial^2}{\partial x^2}+\frac{i}{c}A(t)\frac{\partial}{\partial x}+W(x)\right]\Psi(x,t) \quad (1)$$

by making the Floquet ansatz:

$$\Psi(x,t)=e^{-i\mathcal{E}t}\sum_N e^{-iN\omega t}\psi_N(x) . \quad (2)$$

The harmonic components $\psi_N(x)$ satisfy the system of coupled equations

$$\left[\mathcal{E}+N\omega+\frac{1}{2}\frac{d^2}{dx^2}-W(x)\right]\psi_N(x) = V_+\psi_{N-1}(x)+V_-\psi_{N+1}(x) , \quad (3)$$

where the operators V_+ and V_- are defined by the equation

$$\frac{i}{c}A(t)\frac{d}{dx}=V_+e^{-i\omega t}+V_-e^{i\omega t} . \quad (4)$$

We are interested in solutions that are regular at the origin, and behave at large distances, outside the range of $W(x)$, as

$$\psi_N(x)\sim\sum_M f_{NM}(\mathcal{E})\exp(ik_M x), \quad x\gg 0 \quad (5)$$

with

$$k_M=[2(\mathcal{E}+M\omega)]^{1/2} . \quad (6)$$

The ranges of photon indices N and M are the same in Eqs. (3) and (5). As mentioned in the Introduction, the choice of the branch of the square-root function in Eq. (6) for the various k_M determines whether the solution corresponds to a dominant pole or to a shadow pole of the scattering matrix. We take as our one-dimensional potential and field the same as in Ref. 6; the potential is Gaussian:

$$W(x)=-0.63\exp(-x^2/2.65^2), \quad -\infty<x<+\infty . \quad (7)$$

This potential supports three bound states, the ground state [denoted by (0)] and two excited states [(1) and (2)], the second of which lies extremely close to the continuum threshold ($E_0=-0.4451$, $E_1=-0.1400$, $E_2=-0.000\,14$). The field has an angular frequency $\omega=0.0925$, its intensity I being variable. We expand each harmonic component on a basis set of real square-integrable functions, $\phi_n(x)$, which can represent the short-range part of the wave function, within the range of the potential, supplemented by a set of continuum functions $b(k_M;x)$ which have the appropriate asymptotic form. More explicitly, we write

$$\psi_N(x)=\sum_n c_{Nn}\phi_n(x)+\sum_M d_{NM}b(k_M;x) . \quad (8)$$

We took the ϕ_n to be harmonic-oscillator eigenfunctions,

$$\phi_n(x)=N_nH_n(\lambda x)e^{-\lambda^2x^2/2} , \quad (9)$$

where λ is real and positive, H_n are the Hermite polynomials, and N_n a normalization constant. (Only functions ϕ_n of the appropriate parity are included in the expansion for each ψ_N.) The continuum functions b are, for $x>0$

$$b(k_M;x)=e^{ik_Mx}\Theta(x) , \quad (10)$$

with

$$\Theta(x)=\exp[-1/(e^{x/a}-1)^2] . \quad (11)$$

$\Theta(x)$ is a cutoff function that is zero for $x\to 0$, small within the range of the potential (where the set of the ϕ_n functions is "complete"), and unity outside the range of the potential. For $x<0$, $b(k_M;x)=\pm b(k_M;-x)$, depending on the parity of the $\psi_N(x)$. The cutoff function provides a smooth connection at $x=0$.

The Schrödinger equation (3) is transformed into a matrix eigenvalue equation by projecting it onto the basis functions, without complex conjugation. This operation gives rise to matrix elements involving a product of two b functions, $b(k_{M'};x)b(k_M;x)$, such as

$$\int_{-\infty}^{\infty}dx\, b(k_{M'};x)(\mathcal{E}+N\omega)b(k_M;x) , \quad (12)$$

that do not formally converge if $\mathrm{Im}(k_{M'}+k_M)\le 0$. They can be defined as the analytic continuation of their algebraic expression for $\mathrm{Im}(k_{M'}+k_M)>0$ to the region

$\mathrm{Im}(k_{M'}+k_M)\leq 0$ (see, for example, Ref. 11). It is therefore useful to choose an expression such as (11) for the cutoff function, since $\Theta(x)$ can in this case be expanded in a series of powers of $\exp(-x/a)$, which converges rapidly at large distances.

The interesting eigenvalues and eigenvectors are calculated by the inverse iteration method. Finding the Floquet eigenvalues now comprises finding the correct k_M of Eq. (5), such that the output from the inverse iteration process, $\bar{\mathcal{E}}$, is equal to $k_0^2/2$. One can thus try to minimize the quantity $|\bar{\mathcal{E}}-k_0^2/2|^2$, but problems arise when the numerical calculation converges to a local minimum of $|\bar{\mathcal{E}}-k_0^2/2|^2$ which is not a true zero; it is often necessary to have the input wave numbers k_M very close to their correct values for achieving convergence. Good starting values were easy to choose in our case, from the quasienergies reported by Bardsley, Szöke, and Comella[6] for intensities at which they correspond to dominant poles; we have no difficulty reproducing their results. We followed the trajectories of these eigenvalues towards their zero-field limits by gradually changing the strength of the field.

III. RESULTS

We present our results in Figs. 1 and 2 in a format similar to that of Fig. 11 of Ref. 6, to allow for a direct comparison. Although we performed our calculations in the velocity $(\mathbf{p}\cdot\mathbf{A})$ gauge with the $\mathbf{A}^2$ term removed, we added the ponderomotive energy to the Floquet energies. Thus the threshold appears to shift upwards (see the bold lines in Figs. 1 and 2) linearly with intensity. Also, as the Floquet energies are defined only modulo ω, we can transpose the real parts of all Floquet energies into the interval from 0 to $\omega(=0.0925)$. We note, though, that the parity of the state shifted by $n\omega$ is $P_n=P_0(-1)^n$, where P_0 is the parity of the field-free bound state.

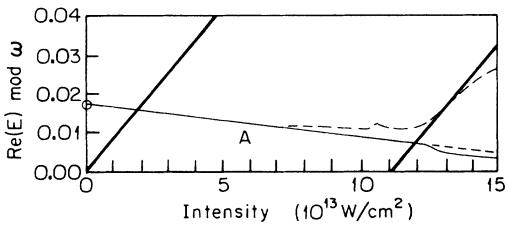

FIG. 1. Real part of the Floquet energy of three poles (forming state *A*) connected to the ground state, as a function of field intensity. The energies are shifted into the interval $0\leq \mathrm{Re}(E)\leq\omega$, and the ponderomotive energy has been added; a threshold thus appears as a straight bold line with positive slope. As the curves stay within the interval $0<\mathrm{Re}(E)<0.04$, the picture has been drawn only for this interval. The three curves are indistinguishable up to an intensity of 6×10^{13} W/cm^2, when the pole that was dominant at small intensities (which now is a shadow pole; its curve is denoted by — — —) starts to move away from the other two poles. These other two poles finally separate, but only slightly, after they cross the second threshold. Here the shadow pole (which was dominant at intermediate intensities) is denoted by - - - -.

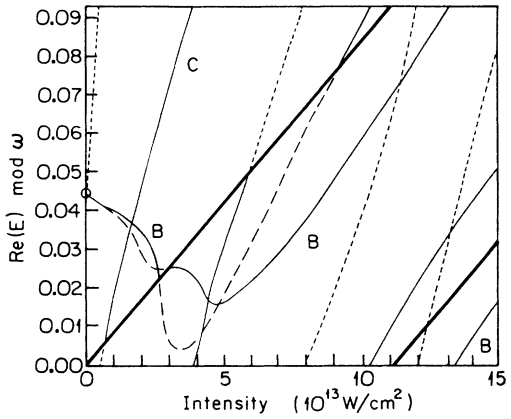

FIG. 2. Real part of the Floquet energy of three poles (forming states *B* and *C*) connected to the first excited state, as a function of field intensity. A bold line denotes a threshold. A dominant pole is denoted by a solid line. The energies are drawn modulo $\omega(=0.0925)$, therefore a pole that disappears over the top of the graph reappears from the bottom at the same intensity. One sees the interchange of roles (dominant vs shadow) of the two poles forming state *B* around $I_{3C}=3\times10^{13}$ W/cm^2.

The authors of Ref. 6 find five different states in their calculations, denoted by *A* through *E* in their Fig. 11. Two of these are continuously connected to the zero-field eigenvalues of the lowest two bound states [$A\rightarrow(0)$, and $B\rightarrow(1)$]. The other three states (*C*, *D*, and *E*) appear as "additional Floquet states" for a certain intensity range. We investigated the movement of the energies of these states as a function of laser intensity, by following the trajectories of the poles on their respective sheets on the energy Riemann surface.

Let us first look at state *A* (see Fig. 1): It crosses two thresholds (downwards, at $I_{1C}=2\times10^{13}$ W/cm^2, and at $I_{2C}=12\times10^{13}$ W/cm^2). At each of these crossings a shadow pole exchanges its status with a dominant pole (see also Fig. 3). Thus we have three poles to follow: the first one is dominant for $0\leq I\leq I_{1C}$, the second one will be dominant for $I_{1C}\leq I\leq I_{2C}$, and the third one for I above I_{2C}. We see that their real parts lie close together. Nevertheless, there are certain differences, and the poles (dominant and shadow) do not cross the threshold at exactly the same intensity nor do they have similar imaginary parts at threshold.

This fact is much more visible in Fig. 2; let us look at state *B*: it crosses only one threshold (downwards, at $I_{3C}\approx3\times10^{13}$ W/cm^2), then turns around and moves roughly parallel to the threshold. This state, therefore, is formed by a dominant pole and a shadow pole, which exchange roles around I_{3C}, and move rather differently for larger intensities. In particular, we see in Fig. 2 that for I above 9×10^{13} W/cm^2 the pole that formed state *B* at small intensities (i.e., that was dominant at zero field) crosses the threshold *upwards* and thus again becomes a dominant pole. This last additional pole was not reported in Ref. 6; it would be seen only for relatively large rotation angles of the complex-coordinate rotation.

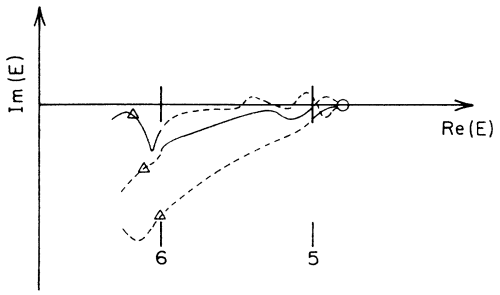

FIG. 3. Schematic sketch of the trajectories of some poles connected to the ground state (the same poles as shown in Fig. 1) in the complex energy plane. For the sake of clarity, the imaginary parts are not drawn to scale, thus the Im(E) axis has no units. The various poles appear to be close to each other but in fact are on different sheets of a multisheeted Riemann surface. A dominant pole is drawn as a solid line; as it crosses a threshold for N-photon detachment (indicated by the short vertical lines, $N=6,5$) it becomes a shadow pole and is drawn as a dashed line. The markers on the trajectories indicate the position of the pole for a certain intensity (in units of 10^{13} W/cm^2): ○ represents 0.0; □ represents 4.0 (only in Fig. 4); △ represents 13.0.

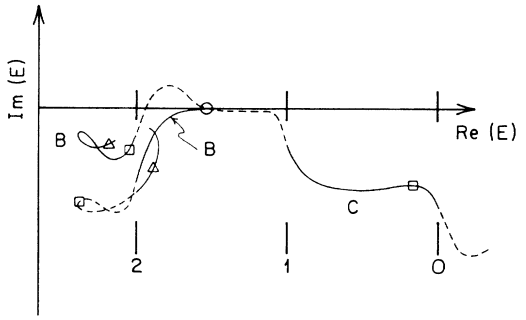

FIG. 4. Schematic sketch of the trajectories of some poles connected to the first excited state (the same poles as shown in Fig. 2) in the complex energy plane. See Fig. 3. $N=2,1,0$ here.

Now we follow the pole denoted as state C (still on Fig. 2) towards smaller intensities. It crosses the threshold (*downwards* for decreasing intensity, that is *upwards* for increasing intensity) at $I_{4C}=1\times10^{13}$ W/cm^2, and changes from a dominant pole to a shadow pole, that finally ends up at the energy (and correct parity) of the first excited bound state (1) at $I=0$. This means that state C is just the appearance of one of the shadow poles connected to state (1). This particular shadow pole happens to move in quite a different direction on the energy surface than its two partner poles that form the state B (Fig. 4), and therefore it becomes, for intensities $I_{4C}\le I\le I_{5C}=6\times10^{13}$ W/cm^2, a dominant pole at an unexpected energy, in addition to the dominant pole forming state B.[12]

We also tried to follow the poles of states D and E to intensities below which they become shadow poles, but we could not find their zero-field limits; we were unable to follow state E below $I=6\times10^{13}$ W/cm^2 (after its real part showed two avoided crossings, and its imaginary part became large and positive), while state D seemed to acquire a large negative imaginary part of the energy for $I\to0$. Also, it was not possible to follow the poles originating from the second excited state (2) towards larger field intensities, because their energy moved extremely close to zero.

Figures 3 and 4 show the trajectories in the complex energy plane of the poles shown in Figs. 1 and 2 (not quite to scale, for the sake of clarity; therefore the Im(E) axis has not been given a scale). The field intensity is indicated by markers on the curves. The trajectories trace rather intricate paths; the curve of the pole forming the first excited state at small I (in Fig. 4) stays on the same sheet of the Riemann surface and intersects itself at larger intensities. The same is true for the curve forming state B at large I. The intersections of the different shadow poles connected to the ground state (Fig. 3), in contrast, are *not* true intersections, as these poles are on different sheets of the Riemann surface. These poles, and one of the poles forming state B, have *positive* imaginary parts for some intensities, but only in regions where they are shadow poles, and therefore not physically observable. That shadow poles could move onto the upper half plane has been observed before in the case of a zero-range potential.[4,13] The pole forming state A at large intensities, which is a shadow pole for $I<I_{2C}$, is allowed to and indeed does pass *above* the threshold for five-photon detachment. Therefore, at very small intensities, the position of this pole is quite remote from the physical energy axis. We see that the paths taken by poles on the multisheeted energy surface, as they move away from the physical energy axis, can be rather complicated.

ACKNOWLEDGMENTS

The authors wish to thank Professor R. Shakeshaft for very helpful discussions. This work was supported by the National Science Foundation under Grant No. PHY-8713196, and by the Faculty Research and Innovation Fund at the University of Southern California.

*Present address: Physics Department, University of Durham, Science Laboratories, South Road, Durham, DH1 3LE, England.

[1]R. J. Eden and J. R. Taylor, Phys. Rev. **133B**, 1575 (1964).
[2]Y. Fujii and M. Fukugita, Nucl. Phys. **B85**, 179 (1975).
[3]P. G. Burke, J. Phys. B **1**, 586 (1968).
[4]V. N. Ostrovskii, Teor. Mat. Fiz. **33**, 126 (1977) [Theor. Math. Phys. **33**, 923 (1977)].
[5]R. M. Potvliege and R. Shakeshaft, Phys. Rev. A **38**, 6190 (1988).
[6]J. N. Bardsley, A. Szöke, and M. J. Comella, J. Phys. B **21**, 3899 (1988).
[7]R. Bhatt, B. Piraux, and K. Burnett, Phys. Rev. A **37**, 98 (1988).

[8]J. N. Bardsley and B. R. Junker, J. Phys. B **5**, L178 (1972).
[9]R. M. Potvliege and R. Shakeshaft, Phys. Rev. A **38**, 1098 (1988).
[10]R. M. Potvliege and R. Shakeshaft, Phys. Rev. A **40**, 3061 (1989).
[11]A. D. Isaacson, C. W. McCurdy, and W. H. Miller, Chem. Phys. **34**, 311 (1978).
[12]This state, and one of the poles associated with state *B*, are examples of shadow poles becoming dominant poles by crossing the threshold *upwards* as the intensity increases. This situation is opposite to the usual one where the poles cross the threshold downwards as the intensity increases, but this peculiar behavior has also been found in the photoionization of atomic hydrogen: see Fig. 3 of Ref. 10, where the curves 4 and 19 are dominant poles that suddenly appear above a certain field strength.
[13]H. G. Muller (private communication).